0023-6837/01/8101-005$03.00/0
LABORATORY INVESTIGATION
Vol. 81, No. 1, p. 5, 2001
Printed in U.S.A.

Effect of Angiogenic and Antiangiogenic Compounds on the Outgrowth of Capillary Structures from Fetal Mouse Bone Explants

Martine Deckers, Gabri van der Pluijm, Saskia Dooijewaard, Marielle Kroon, Victor van Hinsbergh, Socrates Papapoulos, and Clemens Löwik

Department of Endocrinology and Metabolic Diseases (MD, GvdP, SD, SP, CL), Leiden University Medical Center, and Gaubius Laboratory TNO-PG (MK, VvH), Leiden, The Netherlands

SUMMARY: Fetal mouse metatarsals are well-known models to study cartilage differentiation and osteoclastic resorption. We show here the outgrowth of PECAM-1 positive tubelike structures from the bone rudiments. This feature can be used to study angiogenesis in vitro. The area of outgrowth significantly increased with culture time, as shown by computerized image analysis of PECAM-1 positive tubelike structures. Treatment with recombinant human vascular endothelial growth factor (rhVEGF-A) stimulated the formation of tubelike structures. Treatment of explants with the angiogenesis inhibitor endostatin, the chemokine IP-10, and the thalidomide derivative phatolyl glutamic acid (PG-acid) resulted in an inhibition of the formation of PECAM-1 positive tubelike structures of 48.8% (± 4%), 50.2% (±12%), and 80.8% (±3%), respectively. Outgrowth of tubelike structures was partly dependent on endogenous VEGF-A because treatment with anti-mVEGF-A and truncated VEGF receptor 1 (soluble fms-like tyrosine kinase 1, sFlt1) strongly inhibited the formation of tubelike structures 74% (± 4%) and 38% (± 5%), respectively. Neither onset of tube formation nor total area of tubelike structures were changed when metatarsals were cultured on a fibrin gel or collagen type I gel. Tube formation required activation of matrix metalloproteinases because treatment of the bones with an inhibitor of matrix metalloproteinases completely inhibited migration and tube formation, whereas treatment with an inhibitor of plasmin had no effect. In conclusion, we describe a new in vitro model to study angiogenesis that can be used to test the angiogenic or antiangiogenic potential of novel test compounds that also combines the multicellularity of in vivo assays with the accessibility and flexibility of in vitro assays. (*Lab Invest 2001, 81:5–15*).

Angiogenesis, the development of vessels from preexisting vessels, is essential for a variety of physiologic processes, including organ development (Adams et al, 1999; Erlebacher et al, 1995), wound healing, and reproduction (Nissen et al, 1998; Tamura and Greenwald, 1987). In adults it is usually related to pathologic conditions such as rheumatoid arthritis, diabetic retinopathy, tumor progression, and metastasis (Ellis and Fidler, 1996; Folkman, 1995). Highly vascularized tumors are often associated with poor prognosis (Szabo and Sandor, 1998). The identification of circulating antiangiogenic factors in tumor-bearing animals and humans (Fidler and Ellis, 1994; O'Reilly et al, 1997; Sten-Linder et al, 1999) led to the postulation that the activation state of endothelial cells is determined by the balance between endogenous angiogenic and antiangiogenic factors. This implies that if levels of inhibitors are sufficiently high, the angiogenic response will be switched off. This might enable interventions of tumor progression by the use of antiangiogenic compounds (Hanahan and Folkman, 1996); eg. directed against endothelial growth factors, growth factor receptors, proteolytic enzymes, or extracellular matrix molecules (Fisher et al, 1994; Ingber, 1992; Millauer et al, 1994). On the other hand, proangiogenic therapy may provide a promising strategy for patients suffering from vascular insufficiency (Rosengart et al, 1999).

To study the process of angiogenesis and to test new agents with (anti)-angiogenic potential, suitable assays are essential. The most commonly used in vivo assays are the corneal micropocket assay, the chorioallantoic membrane (CAM) assay, and the dorsal skin-fold assay (Fournier et al, 1981; Jakob et al, 1978; Kenyon et al, 1996). To study the efficacy of angiogenic compounds, the corneal micropocket assay, which consists of an avascular environment, is often used. The efficacy of antiangiogenic compounds in inhibiting growth factor induced-vascularization or spontaneous vascularization is usually studied in a vascular environment such as the CAM assay or in the dorsal skin-fold assay. Although these assays have proven their use, they have limitations (for a review see Jain et al, 1997): (a) complicated surgical techniques are required; (b) the number of test compounds that can be assayed for example, in the micropocket assay, is limited; and (c) simultaneous assessment of both angiogenic and antiangiogenic compounds in the same assay without the addition of exogenous growth

Received April 10, 2000.
Address reprint requests to: Dr. Clemens Löwik, Endocrinology and Metabolic Diseases, Leiden University Medical Center, Albinusdreef 2, Building 1, C4R-9, 2333 ZA Leiden, The Netherlands. E-mail: C.W.G.M. Lowik@lumc.nl

factors is not feasible. Most in vitro assays used are based on the assessment of proliferation (Gospodarowicz et al, 1978) or migration of endothelial cells (Nicosia and Ottinetti, 1990; Yamaguchi et al, 1999; Zetter, 1980), but lack nonendothelial cells such as macrophages that are known to contribute markedly to the angiogenic response in vivo (Salvesen and Akslen, 1999). Furthermore, to study tube formation, primary endothelial cells or endothelial cell lines often require a coating of extracellular matrix components (Koolwijk et al, 1996; Montesano et al, 1985). We describe here an in vitro angiogenesis assay, using fetal mouse long bones, in which the multicellularity of in vivo assays is combined with the flexibility of in vitro systems without requiring complicated surgical techniques. Furthermore, we show that the formation of tubelike structures can be assessed without the need of exogenous growth factors or a coating of extracellular matrix molecules, and that the response to inhibitors or stimulators of angiogenesis can be measured quantitatively by image analysis.

Results

Identification of Endothelial Cells

Metatarsals from 17-day-old fetal mice were dissected, fixed, and processed for paraffin embedding. In these sections endothelial cells were identified using PECAM-1 staining (Fig. 1A) and collagen IV staining (data not shown). As expected, at this developmental stage PECAM-1 positive endothelial cells were located in the perichondrium (Fig. 1A). No staining was observed in sections in which the primary antibody was omitted (Fig. 1B) or when an irrelevant rat antimouse monoclonal antibody was used (not shown). The endothelial-specific staining located at the membranes of endothelial cells was confirmed in both frozen and paraffin sections of fetal lung (not shown).

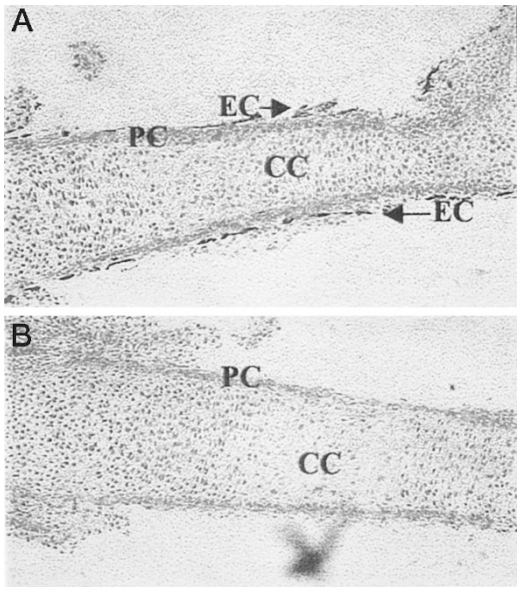

Figure 1.
Localization of endothelial cells in E17 metatarsals. A, Section of dissected E17 mouse metatarsal stained for PECAM-1. Note the endothelial cells in the perichondrium (*arrows*). Original magnification, ×200. B, Control section in which the primary antibody was omitted. *EC*, endothelial cells; *PC*, perichondrium; *CC*, calcifying cartilage.

To study the fate of the endothelial cells, dissected metatarsals were cultured for 14 days. Within 72 hours of culture, the metatarsals had adhered to the culture well due to adhesion of fibroblast-like cells to the culture well. These fibroblast-like cells subsequently started to migrate away from the bone explant. After 5 to 6 days of culture, a resorption cavity was formed, due to osteoclastic activity, which expanded during culture leaving eventually only the cartilage ends (Fig. 2A). After 7 days of culture, formation of tubelike structures over the fibroblast-like cells was observed. These tubelike structures stained positively for PECAM-1. After 10 to 14 days of culture, a densely branched network of PECAM-1 positive tubelike structures (Fig. 2B) on a monolayer of PECAM-1 negative fibroblast-like cells was formed (Fig. 2C). In cultures in which the primary antibody was omitted, staining was not observed (Fig. 2A).

Quantification of Tubelike Structures

Computerized image analysis of cultures after 7, 10, 12, or 14 days of culture showed a significant increase in the formation of PECAM-1 positive tubelike structures from Day 10 on. Similar to the unskeletonized image (number of pixels per area), the skeletonized area (total vessel length), number of endpoints, and number of crosspoints were significantly increased after 10 days of culture (Table 1). The increase in complexity of the network correlated with the increase in area of outgrowth, whereas the number of endpoints increased slightly. When metacarpals instead of metatarsals were used, a similar pattern of outgrowth was observed. However, the overall outgrowth, as indicated by total number of pixels per area, was lower (Fig. 3).

Formation of PECAM-1 Positive Tubelike Structures

Effect of Serum. To determine whether the presence of serum is necessary for the formation of tubelike structures, metatarsals were cultured in the presence of 10% FCS to promote attachment to the culture well. After 72 hours of culture, the medium was replaced by medium containing 1% or 10% FCS, respectively, for 14 days. A decrease in serum concentration strongly inhibited the formation of tubelike structures from 57,060 $\pm$ 3812 pixels per area (10% FCS) to 6539 $\pm$ 306 pixels per area (1% FCS). It should be noted that metatarsals cultured in the presence of 1% serum during the first 72 hours failed to attach to the culture well. Therefore in all experiments described, unless stated otherwise, medium containing 10% FCS was used throughout the total culture period.

Effect of Exogenous rhVEGF-A. Treatment of metacarpals with two doses of exogenous recombinant human vascular endothelial growth factor (rhVEGF-A)

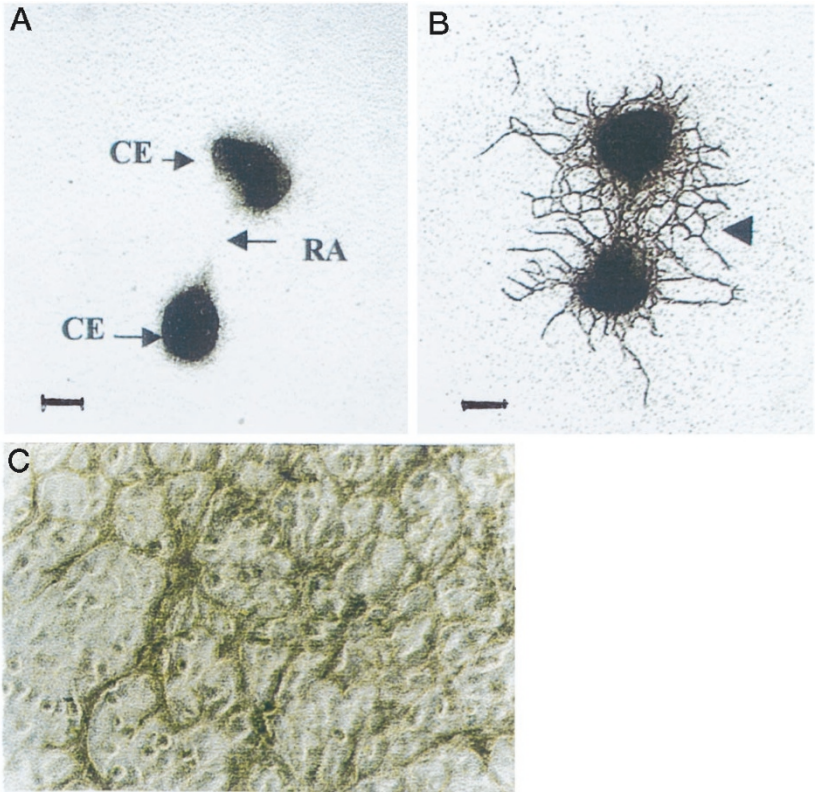

Figure 2.
Formation of tubelike structures. A, Unstained metatarsal after 14 days of culture. Note the formation of a resorption cavity (*arrow*). *RA*, resorbed area; *CE*, cartilage ends. Original magnification, ×40; bar = 1 mm. B, PECAM-1 staining of a metatarsal after 14 days of culture. PECAM-1 positive tubelike structures are indicated by *arrowhead*. Original magnification, ×40; bar = 1 mm. C, Formation of tubelike structures after 10 days of culture. PECAM-1 positive tubelike structures on a monolayer of PECAM-1 negative fibroblast-like cells. Original magnification, ×4000.

Table 1. Quantification of Immunohistochemical Staining by Computerized Image Analysis

Days of culture	Unskeletonized area (pixels/area)	Skeletonized area (pixels/area)	Crosspoints (number of pixels)	Endpoints (number of pixels)
7	24098 ± 29	7810 ± 2083	807 ± 164	197 ± 31
10	27284 ± 4247	10528 ± 1267	788 ± 282	350 ± 82
12	41904 ± 3880	13328 ± 450	1323 ± 144	386 ± 40
14	63484 ± 6198	20095 ± 2240	1835 ± 331	450 ± 74

Seventeen-day fetal mouse metatarsals were cultured for 7, 10, 12, or 14 days. At the timepoints indicated, cultures were fixed and stained for platelet-endothelial cell adhesion molecule-1 (PECAM-1). Capillary outgrowth determined from quadruple cultures was quantified by computerized image analysis as described in "Materials and Methods." The area of outgrowth in unskeletonized images was represented by the mean number of pixels per area (unskeletonized area). After the skeletonizing procedure, the total vessel length was indicated by the mean number of pixels per area (skeletonized area). The complexity of the vascular network was determined by the number of crosspoints and endpoints. Data are expressed as mean ± SEM, $n = 6$ of triplicate experiments. A strong correlation between the unskeletonized area of outgrowth and the crosspoints ($r = 0.9$) and total vessel length ($r = 0.93$) was found.

(10 or 100 ng/ml) resulted in a significant stimulation of the total area of outgrowth, as depicted in Figure 3A. Representative images of PECAM-1–stained control and VEGF-A–treated bones are shown in Figure 3B. Similarly, using the skeletonizing procedure, treatment with VEGF dose-dependently and significantly increased the number of crosspoints as well as the number of endpoints (not shown). This response was specific, because treatment with a functional blocking antibody directed against human VEGF (anti-hVEGF) reversed the effect, whereas a functional blocking antibody directed against antimouse VEGF-A had no effect (Fig. 3C). It should be noted that antihuman VEGF antibody had no effect on basal outgrowth. In the presence of 1% FCS, similar to the control cultures (see above), treatment with rhVEGF-A did not result in a significant induction of tubelike structures (120% ± 10%).

The Role of Endogenous VEGF-A. To determine whether endogenous mouse VEGF-A was required for the formation of PECAM-1 positive tubelike structures, cultures were treated with a functional blocking antibody directed against mouse VEGF-A (anti-mVEGF-A) or with truncated VEGF receptor 1 (soluble fms-like tyrosine kinase 1, sFlt1) (Roeckl et al, 1998). Treatment with anti-mVEGF-A from Day 7 to Day 14

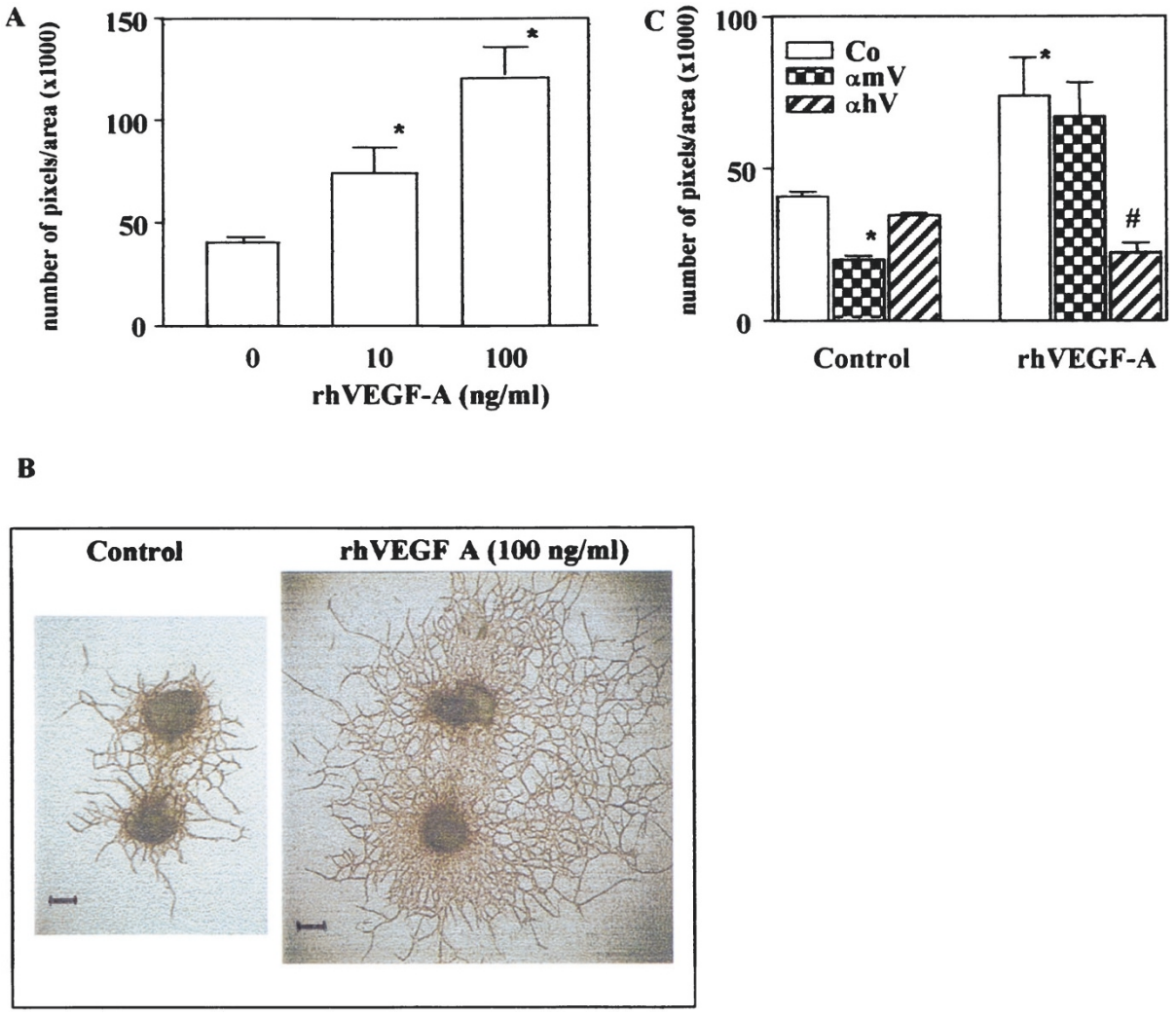

Figure 3.

Effect of rhVEGF-A on the formation of PECAM-1 positive tubelike structures. A, Fetal mouse metacarpals were treated with 10 or 100 ng/ml rhVEGF-A. After 14 days of culture, the number of PECAM-1 positive pixels per area was quantified. rhVEGF-A dose-dependently and significantly stimulated the formation of tubelike structures. * $p < 0.05$ as compared with controls, $n = 6$. B, Representative images of PECAM-1 staining of control and VEGF-treated (100 ng/ml) cultures after 14 days of culture (bar = 1 mm). C, Species-specific inhibition of VEGF-A–induced tube formation. Metacarpals were treated with rhVEGF-A (10 ng/ml) in absence or presence of antimouse VEGF-A antibody (anti-mVEGF-A; 1 μg/ml) or antihuman VEGF-A antibody (anti-hVEGF-A; 1 μg/ml) for 14 days. rhVEGF-A–induced tube formation was reversed to control levels by αhV and not by αmV. * $p < 0.05$ as compared with controls; # $p < 0.05$ as compared with rhVEGF-A-treated cultures, $n = 5$. *Co*, control; αmV, anti-mVEGF-A; αhV, anti-hVEGF-A.

resulted in a 40% (± 5%) inhibition of the formation of PECAM-1 positive tubelike structures, as shown in Figure 4. In addition, when the antibody treatment was started at Day 3 of the experiment in the absence of rhVEGF, the formation of PECAM-1 positive tubelike structures was inhibited by 74% (± 4%) (Fig. 3C). In the presence of rhVEGF-A, the anti-mVEGF-A antibody had no effect (Fig. 3C). Treatment with sFlt1 from Day 3 on dose-dependently inhibited the formation of PECAM-1 positive tubelike structures (Fig. 5). Similarly, treatment of metatarsals with a combination of rhVEGF-A and various doses of sFlt1 completely reversed the formation of PECAM-1 positive tubelike structures to control levels (Fig. 5). This suggests that sFlt1 inhibits both human and mouse VEGF-A–induced formation of tubelike structures.

Effect of Recombinant Human Endostatin. To test the angiostatic properties of soluble recombinant human endostatin derived from an embryonic kidney cell line (EBNA 293 cells) (Yamaguchi et al, 1999), metatarsals were treated with recombinant human endostatin (rhEndostatin) or anti-mVEGF-A for comparison (Fig. 6). Treatment with rhEndostatin at a concentration of 1 and 5 μg/ml significantly inhibited the formation of PECAM-1 positive tubelike structures after 14 days of treatment (Fig. 6). Outgrowth of fibroblast-like cells, however, was not blocked by treatment with rhEndostatin, indicating that this agent exerts an endothelial-specific effect. Formation of tubelike structures was also significantly inhibited by treatment with 5 μg/ml recombinant mouse endostatin (not shown).

Effect of PG-Acid and IP-10. To test the angiostatic properties of various classes of antiangiogenic agents, metatarsals were treated with a thalidomide derivative, phatolyl glutamic acid (PG-acid) or the chemo-

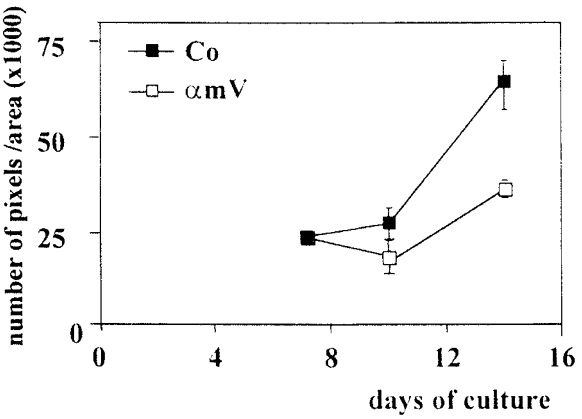

Figure 4.
Effect of a functional blocking antibody against mVEGF-A on the formation of PECAM-1 positive tubelike structures. Metatarsals were treated with antimouse VEGF-A antibody (1 μg/ml) from Day 7 to Day 14 of culture. The number of PECAM-1 positive pixels per area was measured after 10 and 14 days of culture, as described in Figure 3. *Co*, control; *αmV*, anti-mVEGF-A antibody.

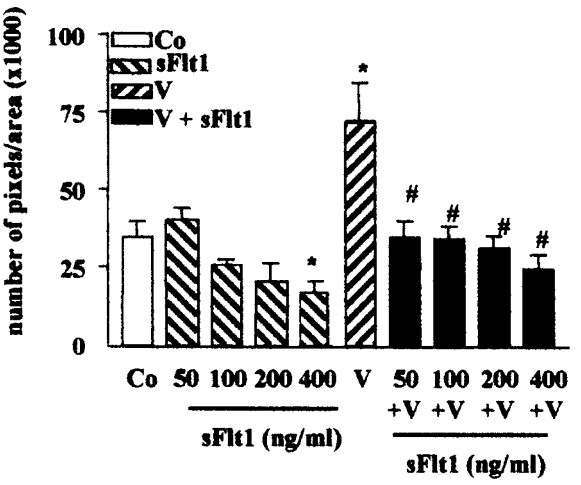

Figure 5.
Effect of soluble Flt1 on the formation of PECAM-1 positive tubelike structures. Fetal mouse metatarsals were treated with various doses of sFlt1 for 14 days in presence or absence of 10 ng/ml rhVEGF-A. The number of PECAM-1 positive pixels per area was determined as described in Figure 3. sFlt1 dose-dependently inhibited the formation of tubelike structures both in the presence and absence of rhVEGF-A. * $p < 0.05$ compared with controls; # $p < 0.05$ compared with VEGF-A–treated cultures, $n = 6$. *Co*, control; *V*, rhVEGF-A.

kine interferon-γ-inducible protein 10 (IP-10), respectively. Treatment of metatarsals with the thalidomide derivative PG-acid for 14 days dose-dependently inhibited the formation of PECAM-1 positive tubelike structures from 33,544 $\pm$ 4325 (control cultures) to 26,338 $\pm$ 3844 (0.1 mg/ml PG-acid), 21,828 $\pm$ 1108 (1 μg/ml PG-acid), and 6,444 $\pm$ 213 (10 μg/ml PG-acid), respectively. In addition, treatment with the chemokine IP-10 resulted in a significant and dose-dependent inhibition of the area of outgrowth (Fig. 7).

Effect of Extracellular Matrix Coatings and Protease Inhibitors. Because other in vitro angiogenesis assays require a coating of extracellular matrix molecules, we compared the number of PECAM-1 positive pixels in cultures grown on a coating of gelatin or on a fibrin gel or collagen type I gel, respectively. On gelatin, formation of tubelike structures was strongly inhibited due to ineffective adhesion of the metatarsal to the gelatin. On collagen type I gel and fibrin gel, however, the onset of tube formation was not different compared with controls and occurred from Day 7 on. After 14 days of culture, the total area of outgrowth was also not different among cultures grown on plastic (67,727 $\pm$ 4232 pixels/area), on a fibrin gel (61,206 $\pm$ 5952 pixels/area), or on a collagen type I gel (58,389 $\pm$ 7722 pixels/area).

To test whether proteinases are involved in tube formation, metatarsals were cultured in the presence of marimastat (10^{-6}M), a broad-spectrum matrix metalloproteinase (MMP) inhibitor, or aprotinin (100 KIE/ml), an inhibitor of plasmin activity, respectively. Treatment with marimastat strongly inhibited the number of PECAM-1 positive pixels per area in cultures grown both on plastic (from 67,727 $\pm$ 4234 to 39,311 $\pm$ 3929 pixels/area) and on a fibrin gel (from 61,206 $\pm$ 5952 to 34,913 $\pm$ 3791 pixels/area). Furthermore, the outgrowth of fibroblast-like cells was inhibited by marimastat. In contrast, treatment with aprotinin had no effect on the number of pixels per area of cultures grown on plastic (69,957 $\pm$ 7900) or on a fibrin gel (72,812 $\pm$ 1460). This suggests that the formation of PECAM-1 positive tubelike structures in our assay acts via an MMP-dependent process rather than a plasmin-dependent process.

Discussion

Fetal long bones of specific developmental stages, representing different stages of endochondral bone formation, are well-known models to study chondrocyte differentiation (E15) (Dieudonne et al, 1994; Haaijman et al, 1999) or osteoclastic resorption (E17) (Van Beek et al, 1993; van der Pluijm et al, 1991). Here we describe the use of E17 mouse metatarsals as a simple and quantitative assay to study the formation of capillary-like structures in response to angiogenic (VEGF) and antiangiogenic factors (endostatin, IP-10, and PG-acid). These tubelike structures exhibited an endothelial-like morphology and expressed the endothelial markers PECAM-1 (CD31) and collagen type IV.

The formation of PECAM-1 positive tubelike structures occurred from Day 7 on. By this time a feeder layer of fibroblast-like cells had formed. This lag time in tube formation might be explained by the need of a feeder layer of fibroblast-like cells on which endothelial cells can migrate. To study whether this feeder layer could be replaced by a coating or a gel consisting of extracellular matrix proteins, thereby accelerating the onset of tube formation, metatarsals were cultured on a coating of gelatin or on a fibrin or collagen gel. In our assay, tube formation did not occur on gelatin-coated dishes due to ineffective adhesion of the metatarsals to the culture well. This is consistent with the finding that endothelial cells cultured on gelatin-coated dishes retain their "cobblestone-like" morphology and fail to organize into tubelike structures. Although enhanced migration and

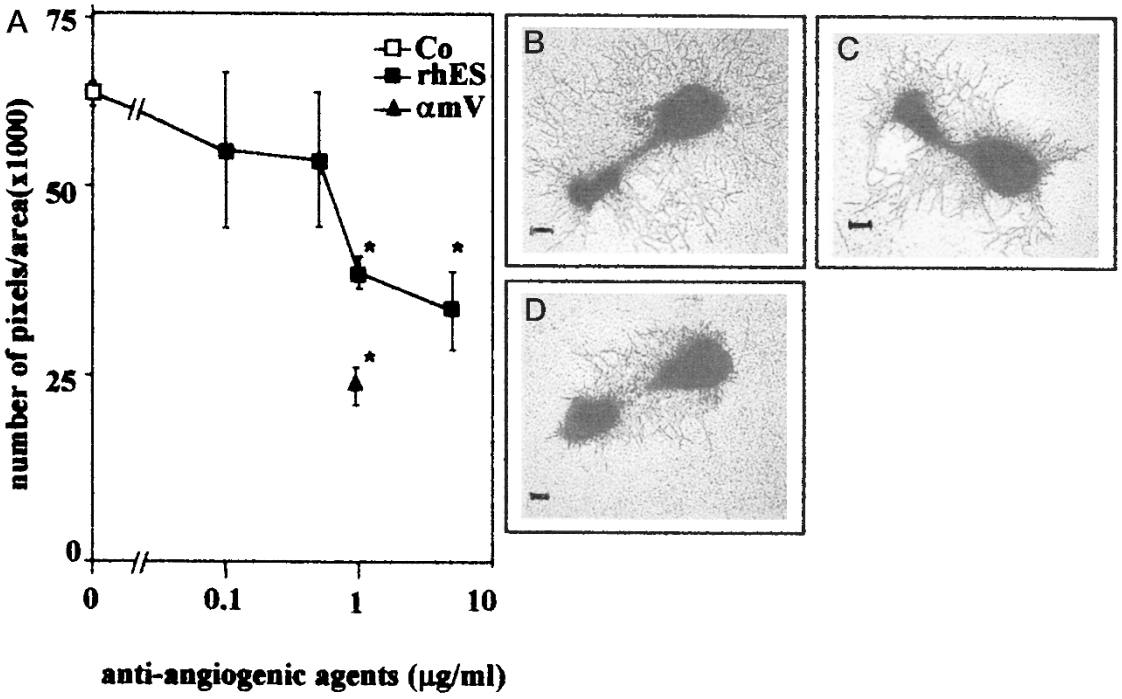

Figure 6.

Effect of rhEndostatin on the formation of PECAM-1 positive tubelike structures. A, Metatarsals were treated with various concentrations of soluble rhEndostatin or 1 μg/ml anti-mVEGF-A for 14 days. Measurement of the number of PECAM-1 positive pixels per area in control cultures (*open squares*), after treatment with endostatin (*solid squares*) or after treatment with 1 μg/ml anti-mVEGF-A (*solid triangle*) after 14 days of culture. Both soluble rhEndostatin and anti-mVEGF-A significantly inhibited formation of tubelike structures. *Co*, control; *ES*, rhEndostatin; α*mV*, anti-mVEGF-A. * $p < 0.05$ compared with controls, $n = 6$. B to D, Representative images of PECAM-1 staining of control explants (B), soluble rhEndostatin (1 μg/ml)-treated explants (C), and anti-mVEGF-A (1 μg/ml)–treated explants (D).

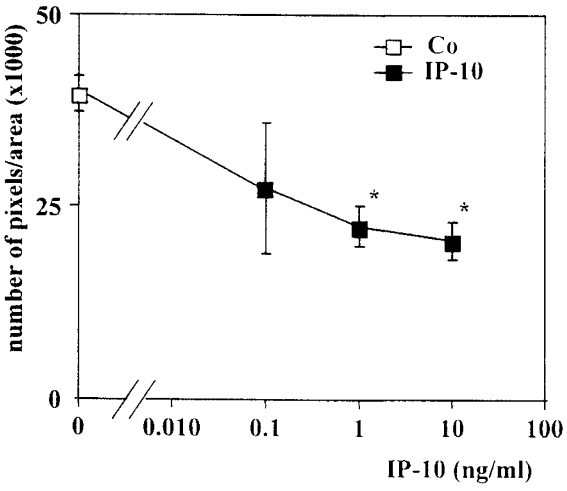

Figure 7.

Effect of IP-10 on the formation of PECAM-1 positive tubelike structures. Metacarpals were cultured in the presence of various concentrations of IP-10. After 14 days of culture, the number of PECAM-1 positive pixels was quantified. IP-10 dose-dependently and significantly inhibited the formation of tubelike structures. * $p < 0.05$ compared with controls, $n = 6$.

tube formation by endothelial cells cultured on collagen, fibrin gels, or Matrigel has been reported in vitro (Koolwijk et al, 1996; Montesano et al, 1985; Nicosia and Ottinetti, 1990), in our experimental conditions the onset of tube formation was not accelerated nor the area of PECAM-1 positive tubelike structures enlarged.

A key feature in the angiogenic process in vivo is degradation of the basement membrane by proteolysis (Pepper and Montesano, 1990), which is mediated by serine proteases, in particular the plasminogen activator/plasmin system, and MMPs (Werb et al, 1999). To examine which class of proteolytic enzymes is involved in tube formation in our assay, cultures were treated with aprotinin (bovine pancreas trypsin inhibitor), an inhibitor of plasmin activity, or marimastat, a synthetic low-molecular-weight MMP inhibitor (Wojtowicz-Praga et al, 1997). Treatment with marimastat attenuated the formation of tubelike structures in cultures grown on plastic, collagen type I, or fibrin gel, which is in agreement with Fisher et al (1994), who showed MMP-dependent inhibition of tube formation in endothelial cells grown on collagen type I. In contrast to other models based on fibrin invasion (Jimi et al, 1995; Koolwijk et al, 1996), treatment with aprotinin did not have an effect on endothelial sprouting, regardless of the type of coating used. Observations in mice deficient for UPA, tPA, or PAI revealed that angiogenesis was not affected at birth, which may be related to the fact that during development fibrin is not a major component of the extracellular matrix (for a review see Pepper, 1997). This might also explain the finding that in our assay the angiogenic response is

not mediated by a plasmin-dependent mechanism but via activation of MMPs.

Spontaneous formation of tubelike structures was mainly dependent on endogenous VEGF-A, because treatment with a functional blocking antibody directed against mouse VEGF-A and sFlt1 strongly inhibited endothelial sprouting. The cellular source of endogenous VEGF production in these fetal long bones is unknown. Macrophages, which are present in large numbers in the cultures, are known to be an important source of VEGF production in tumors (Salvesen and Akslen, 1999). Furthermore the bone explant itself might serve as an important source of endothelial growth factors. We and others have recently shown that VEGF-A, -B, and -D are expressed in fetal long bones as well as in osteoblasts (Aase et al, 1999; Deckers et al, 2000; Dumont et al, 1995). Interestingly, when the capillary outgrowth in rhVEGF-A–stimulated metatarsals was compared with spontaneous outgrowth (controls), the inhibitory effect of anti-hVEGF was stronger and the effect of anti-mVEGF was less than expected. This suggests that the presence of exogenous rhVEGF-A reduced the contribution of endogenous mVEGF-A. It should be noted that the endogenous production of angiogenic growth factors does not restrict the applicability of the assay because treatment with rhVEGF-A stimulated the formation tubelike structures.

The assay was shown to be suitable for testing various classes of angiostatic agents, as shown for the thalidomide derivative PG-acid, the chemokine IP-10, and recombinant endostatin. Similar to previous observations (Kenyon et al, 1997) we show that PG-acid acts as an angiostatic agent. IP-10 is a member of the C-X-C superfamily of chemokines. This family consists of polypeptides that have either proangiogenic or antiangiogenic activity (for a review see Neville et al, 1997). IP-10, which lacks an ELR motif at the NH_2-terminus of the peptide, is considered to be antiangiogenic (Moore et al, 1998). In agreement with previous observations we found that IP-10 acts as a very potent inhibitor of the formation of tubelike structures in vitro (Arenberg et al, 1997; Strieter et al, 1995). We additionally showed angiostatic activity of IP-10 even in the absence of exogenously added growth factors.

Treatment of metatarsals with the 20 kDa angiostatic fragment of collagen 18 (endostatin) attenuated the formation of tubelike structures without affecting the formation of a feeder layer of fibroblast-like cells, underscoring the endothelial-specific properties of this angiostatic agent (Cao, 1998; O'Reilly et al, 1997; Taddei et al, 1999). This is in agreement with other recent studies in which the angiostatic effect of endostatin on endothelial cells was shown in vitro (Dhanabal et al, 1999a, 1999b; Yamaguchi et al, 1999) and in vivo (Dhanabal et al, 1999a; O'Reilly et al, 1997). In contrast to recent observations by Kruger et al (2000) who used the human saphenous vein model and the rat aortic ring model, we did not detect a species difference in the antiangiogenic activity of endostatin. It should be noted that endothelial cells surrounding E17 metatarsals positively stained for collagen XVIII (own unpublished results), the endogenous source of mouse endostatin, which might explain the relatively high levels (5 μg/ml) of this agent needed to block the angiogenic response as compared with other in vitro studies (Taddei et al, 1999; Yamaguchi et al, 1999).

Although angiogenesis was inhibited by different classes of angiostatic agents, a small residual angiogenic activity was noticed. This might result from capillaries lining the bone explant present at the time of dissection that grow during the adhesion phase of the experiment when test compounds have not yet been added. Second, residual angiogenic activity might result from the activity of other members of the VEGF growth factor family, other secreted growth factors (PDGF), or matrix-bound factors (TGF-β, or acidic or basic FGF) that compensate for the inactivation of VEGF-A.

In conclusion, we have developed a novel in vitro angiogenesis assay in which the angiogenic as well as the angiostatic potential of various classes of compounds can be tested. Spontaneous tube formation occurred even in the absence of a coating of extracellular matrix proteins and exogenous growth factors. This model combines both the flexibility and accessibility of in vitro models with the complexity of in vivo assays, in particular the contribution of inflammatory cells and stromal cells that interact with endothelial cells. With the growing demand for easy and reproducible in vitro angiogenesis assays and the growing interest in the specific properties of endothelial cells, this assay provides a new tool for screening agents for potential clinical use and further research in the field of angiogenesis.

Material and Methods

Culture of Fetal Metatarsals

Seventeen-day-old fetuses were removed from pregnant Swiss albino mice and metatarsals were subsequently aseptically dissected as previously described (van der Pluijm et al, 1991). At this stage of development, both endothelial cells and osteoclast precursors are located in the perichondrium. The isolated metatarsals were fixed in zinc macrodex formalin (ZnMF) fixative (0.1 M Tris acetate [pH 4.5] containing 0.5% $ZnCl_2$, 0.5% zinc acetate, 5% dextran, and 10% formalin) for 3 hours at room temperature, decalcified in 5% sodium EDTA for 24 hours at 4° C, and subsequently processed for paraffin embedding.

Immunohistochemistry

Immunohistochemistry was performed on 5 μm ZnMF-fixed paraffin-embedded sections of 17-day-old fetal hindlimbs. Sections were rehydrated and washed with phosphate buffered saline (PBS), followed by incubation with 40% methanol/1% H_2O_2 in PBS for 15 minutes to abolish endogenous peroxidase activity. The sections were incubated with 0.5% Boehringer blocking reagent (BMP; Boehringer-Mannheim Biochemica, Mannheim, Germany) in 0.1 M Tris-buffered saline (pH

7.5) containing 0.02% Tween-20 (BMP/TNT) for 1 hour at 37° C. This was followed by incubation with primary rat antimouse antibody ER-MP12 directed against murine PECAM-1 (kindly provided by Dr. P. Leenen, Erasmus University, Rotterdam, The Netherlands) diluted in BMP/TNT for 16 hours at 4° C. Sections were incubated with biotinylated sheep antirat antibody (Amersham, Den Bosch, The Netherlands), diluted in BMP/TNT for 45 minutes at 37° C followed by incubation for 30 minutes with horseradish conjugated streptavidin (strep-HRP; Amersham) diluted in BMP/TNT. The signal was amplified using biotinylated tyramids, as previously described (Kerstens et al, 1995), followed by incubation with strep-HRP, and finally detected by the chromogen 3-amino-9-ethyl-carbazole (AEC; Sigma Chemicals, Zwijndrecht, The Netherlands).

To study the expression of collagen IV, successive sections were incubated overnight in rabbit antirat collagen IV antibody (Brunschwig, Amsterdam, The Netherlands). Signal was amplified using biotinylated donkey antirabbit IgG followed by incubation with strep-HRP and biotinylated tyramids, as described above.

Angiogenesis Assay

Seventeen-day-old fetuses were removed from pregnant Swiss albino mice and metatarsals were dissected. The isolated metatarsals were cultured in 24-well plates in 150 μl minimal essential medium (αMEM; Life Technologies, Breda, The Netherlands) supplemented with 10% (v/v) heat-inactivated fetal bovine serum and penicillin/streptomycin (Life Technologies) for 72 hours. Cultures were performed in sextuple and each experiment was repeated at least twice. After 72 hours (adhesion phase), the metatarsals were attached to the culture plastic and medium was replaced by 250 μl fresh medium in the presence or absence of test compounds: rhVEGF-A (Oncogene, Sanbio, Uden, The Netherlands); anti-mVEGF-A or goat antihuman VEGF-A (anti-hVEGF-A) antibody (R&D Systems, ITK, Uithoorn, The Netherlands); PG-acid, a metabolite of thalidomide (Sigma Chemicals, Zwijndrecht, The Netherlands); or aprotinin (100 KIE/ml; Pentapharm Ltd, Basel, Switzerland). The MMP inhibitor marimastat was kindly provided by Chiroscience Inc. (Cambridge, United Kingdom). Purified recombinant human endostatin (rhEndostatin) was kindly provided by Dr. B. Olsson (Harvard Medical School, Boston). Purified recombinant interferon-γ-inducible protein 10 (IP-10) was kindly given by Dr. C. Tensen (Department of Dermatology, Leiden, The Netherlands). Truncated VEGF receptor 1 or sFlt1 was kindly provided by Dr. H. Weich (National Research Center for Biotechnology, Braunschweig, Germany). Metatarsals were cultured for 7, 10, 12, or 14 days, as indicated, and medium was replaced every 7 days. At the end of the culture period, cultures were fixed in ZnMF fixative for 15 minutes at room temperature and subsequently stained for PECAM-1.

Preparation of Fibrin Coating, Collagen Type I Coating, and Gelatin Coating

Human fibrin coating was prepared as previously described (Kroon et al, 1999). Briefly, 0.1 U/ml thrombin (Organon Technika, Boxtel, The Netherlands) was added to a mixture of 2.5 U/ml factor XIII (final concentrations), 2 mg/ml fibrinogen (Chromogenix AB, Mölndal, Sweden), 2 mg/ml Na-citrate, 0.8 mg/ml NaCl, and 3 μg/ml plasminogen in M199 medium (Life Technologies; mixture pH = 7.4). Aliquots of 100 μl of this mixture were added to the wells and, after clotting at room temperature, the fibrin coating was soaked with M199 supplemented with 10% (v/v) human serum and 10% (v/v) NBCS for 2 hours at 37° C to inactivate the thrombin. Thrombin and factor XIII were generously provided by Dr. H. Boeder and Dr. P. Kappus (Centeon Pharma GmbH, Marburg, Germany).

To prepare the collagen coating, collagen type I was solubilized from adult rat tail tendons as described by Strom and Michalopoulos (1982). Subsequently, 7 volumes of rat collagen type I were mixed with 1 volume of 10$\times$ M199 and 2 volumes of 0.2% $NaHCO_3$ (mixture pH 7.4), giving an end concentration of 3 mg/ml. A volume of 100 μl was added to each well and was allowed to gel at 37° C in the absence of CO_2.

To prepare the gelatin coating, wells were coated with 250 μl 0.1% (v/v) gelatin at 37° C. After 1 hour of incubation, excess liquid was removed. The isolated metatarsals were cultured in 24-well plates in 250 μl αMEM. After 72 hours, the medium was replaced and trasylol (100 KIE/ml) and marimastat (10^{-6}M diluted in DMSO) were added as described above. Cultures containing 0.001% DMSO were used as control.

PECAM-1 Staining of Tubelike Structures

Immunohistochemistry was performed on ZnMF-fixed bone explants. Explants were incubated with 40% methanol/1% H_2O_2 in PBS for 15 minutes to abolish endogenous peroxidase activity. After three washes with PBS, the cultures were incubated with BMP/TNT for 1 hour at 37° C and subsequently incubated with 250 μl ER-MP12 (1:50 diluted in BMP/TNT) for 16 hours at 4° C. This was followed by incubation with biotinylated sheep antirat secondary antibody for 45 minutes at 37° C and strep-HRP for 30 minutes at 37° C. The signal was visualized using the chromogen AEC. The cultures were stored in PBS until image analysis.

Image Analysis

The formation of tubelike structures was measured quanitatively by computerized image analysis. Images were acquired using a color CCD camera mounted on a Nikon Eclipse 610 microscope at a 40-fold magnification. Images of control and treated cultures were digitized with a Matrix meteor frame grabber, filtered and analyzed with Image Pro Plus 3.0 for Windows 95/NT and the "skeletonize" plugin program (Media Cybernetics, Silver Spring, Maryland) (Fig. 8). Control samples from previous experiments were also in-

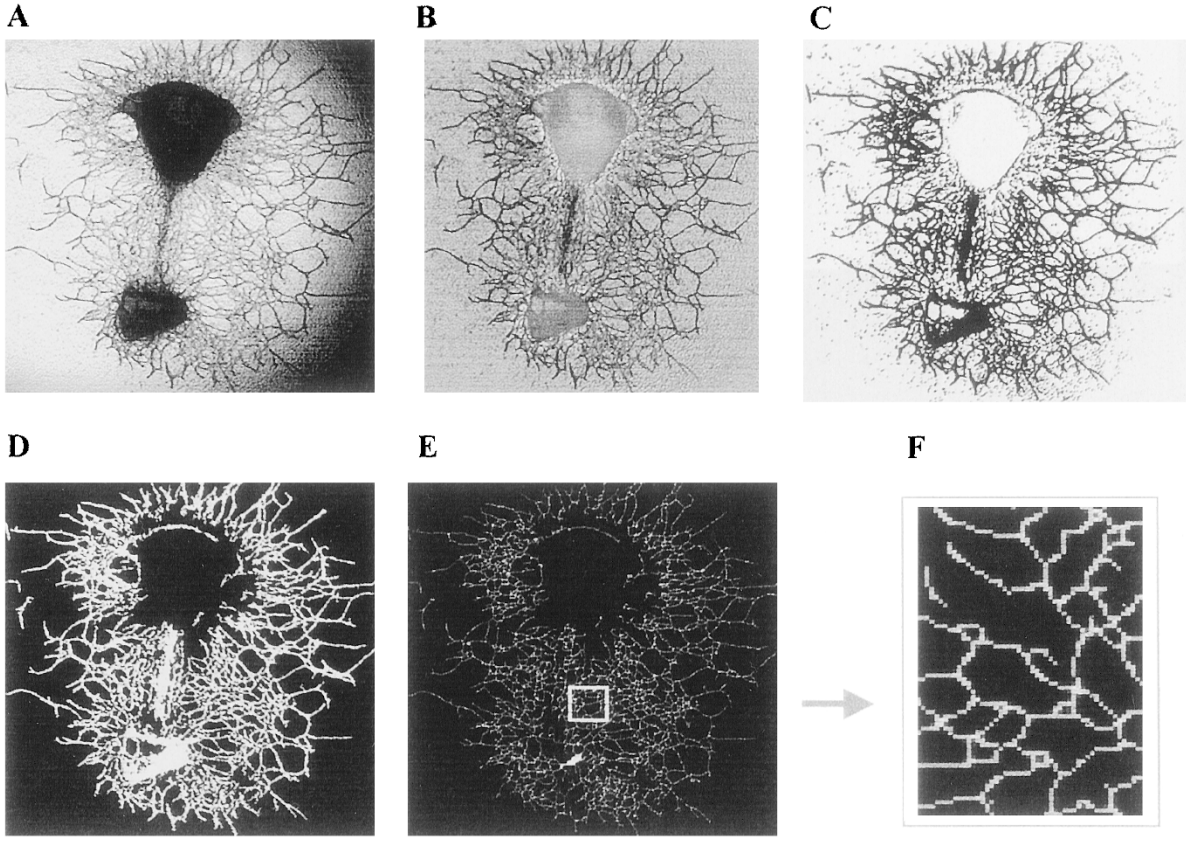

Figure 8.

Image processing. Quantification of the formation of PECAM-1 positive tubelike structures was performed in sequential steps using Image Pro Plus. A, Image captured by CCD camera. B, Image from which background is subtracted and reverted to a grayscale image. C, Binary image after manual adjustment on a scale of 1–255. D, Masked image devoid of cell debris and PECAM-1 negative stromal cells, showing areas > 50 pixels. E, Skeletonized image after thinning and convolution filtering. F, Magnification of area boxed in E: ×40.

cluded in each experiment as references. The images were analyzed in sequential steps as described below (Nissanov et al, 1995).

1. Background Correction. To correct for nonspecific background staining, the bone explant of a control culture was removed without disrupting the network of tubelike structures. In the staining procedure of this control culture the primary antibody was omitted. The image was subsequently acquired and Gaussian smoothed and subtracted from the target image. The obtained image was reverted to a grayscale image representing bone, endothelial cells, and nonendothelial cells (Fig. 8B).

2. Binary Image. The image was binarized and manually adjusted (on a scale of 1–255) so that endothelial cells could be distinguished from the background as connected vessels (Fig. 8C). The level of adjustment was determined for each experiment separately. Differences in intensity of PECAM-1 staining among the different treatment groups were negligible and the level of adjustment was kept fixed. Areas of more than 50 pixels were selected and automatically counted, resulting in a masked image in which only the counted objects are shown (Fig. 8D). The area representing the bone explant was selected by manually drawing a boundary around the bone. The net area of outgrowth was calculated by subtracting the number of white pixels in the area of the explant from the total number of white pixels.

3. Reduction of Image. To quantify the skeletonized area (total vessel length) or complexity of the network (number of crosspoints), the images were reduced to a skeleton of one pixel wide using a thinning filter (1E). This implies that the sum of all pixels is equal to the total vessel length.

4. Convolution Filtering. To quantify the number of crosspoints and the number of endpoints, a unique value was applied to each pixel by convolution filtering. In this procedure, using a matrix of filtering coefficients (kernels) all pixels were given a unique value represented by the grayscale in the skeletonized image (Fig. 8F). Different thresholds on a scale of 150–255 were used to select and count the number of endpoints (1 neighboring pixel, threshold 157), number of crosspoints (3 or more neighboring pixels, threshold 170), or total vessel length (threshold 255). Because a strong correlation was found between the total area of outgrowth, the complexity of the network ($r = 0.90$), and total vessel length ($r = 0.93$), respectively, only the total area is depicted in the graphs. An example of the quantification is given in Figure 8.

Statistics

Results are depicted as mean value ± standard error of the mean (SEM). Differences between groups were determined by one-way analysis of variance for multiple comparison followed by Fisher's LSD test.

References

Aase K, Lymboussaki A, Kaipainen A, Olofsson B, Alitalo K, and Eriksson U (1999). Localization of VEGF-B in the mouse embryo suggests a paracrine role of the growth factor in the developing vasculature. Dev Dyn 215:12–25.

Adams RH, Wilkinson GA, Weiss C, Diella F, Gale NW, Deutsch U, Risau W, and Klein R (1999). Roles of ephrinB ligands and EphB receptors in cardiovascular development: Demarcation of arterial/venous domains, vascular morphogenesis, and sprouting angiogenesis. Genes Dev 13:295–306.

Arenberg DA, Polverini PJ, Kunkel SL, Shanafelt A, and Strieter RM (1997). In vitro and in vivo systems to assess role of CXC chemokines in regulation of angiogenesis. Methods Enzymol 288:190–220.

Cao Y (1998). Endogenous angiogenesis inhibitors: Angiostatin, endostatin, and other proteolytic fragments. Prog Mol Subcell Biol 20:161–176.

Deckers MML, Karperien M, van der Bent C, Yamashita T, Papapoulos SE, and Lowik CWGM (2000). Expression of vascular endothelial growth factors (VEGFs) and their receptors during osteoblast differentiation. Endocrinology 141: 1667–1674.

Dhanabal M, Ramchandran R, Volk R, Stillman IE, Lombardo M, Iruela-Arispe ML, Simons M, and Sukhatme VP (1999a). Endostatin: Yeast production, mutants, and antitumor effect in renal cell carcinoma. Cancer Res 59:189–197.

Dhanabal M, Ramchandran R, Waterman MJ, Lu H, Knebelmann B, Segal M, and Sukhatme VP (1999b). Endostatin induces endothelial cell apoptosis. J Biol Chem 274:11721–11726.

Dieudonne SC, Semeins CM, Goei SW, Vukicevic S, Nulend JK, Sampath TK, Helder M, and Burger EH (1994). Opposite effects of osteogenic protein and transforming growth factor beta on chondrogenesis in cultured long bone rudiments. J Bone Miner Res 9:771–780.

Dumont DJ, Fong GH, Puri MC, Gradwohl G, Alitalo K, and Breitman ML (1995). Vascularization of the mouse embryo: A study of flk-1, tek, tie, and vascular endothelial growth factor expression during development. Dev Dyn 203:80–92.

Ellis LM and Fidler IJ (1996). Angiogenesis and metastasis. Eur J Cancer 32A:2451–2460.

Erlebacher A, Filvaroff E, Gitelman SE, and Derynck R (1995). Toward a molecular understanding of skeletal development. Cell 80:371–378.

Fidler IJ and Ellis LM (1994). The implications of angiogenesis for the biology and therapy of cancer metastasis. Cell 79: 185–188.

Fisher C, Gilbertson-Beadling S, Powers EA, Petzold G, Poorman R, and Mitchell MA (1994). Interstitial collagenase is required for angiogenesis in vitro. Dev Biol 162:499–510.

Folkman J (1995). Angiogenesis in cancer, vascular, rheumatoid and other disease. Nat Med 1:27–31.

Fournier GA, Lutty GA, Watt S, Fenselau A, and Patz A (1981). A corneal micropocket assay for angiogenesis in the rat eye. Invest Ophthalmol Vis Sci 21:351–354.

Gospodarowicz D, Greenburg G, Bialecki H, and Zetter BR (1978). Factors involved in the modulation of cell proliferation in vivo and in vitro: The role of fibroblast and epidermal growth factors in the proliferative response of mammalian cells. In Vitro 14:85–118.

Haaijman A, Karperien M, Lanske B, Hendriks J, Lowik CW, Bronckers AL, and Burger EH (1999). Inhibition of terminal chondrocyte differentiation by bone morphogenetic protein 7 (OP-1) in vitro depends on the periarticular region but is independent of parathyroid hormone-related peptide. Bone 1999 25:397–404.

Hanahan D and Folkman J (1996). Patterns and emerging mechanisms of the angiogenic switch during tumorigenesis. Cell 86:353–364.

Ingber D (1992). Extracellular matrix as a solid-state regulator in angiogenesis: Identification of new targets for anti-cancer therapy. Semin Cancer Biol 3:57–63.

Jain RK, Schlenger K, and Yuan F (1997). Quantitative angiogenesis assays: Progress and problems. Nat Med 3:1203–1208.

Jakob W G, Jentzsch KD, Mauersberger B, and Heder G (1978). The chick embryo choriallantoic membrane as a bioassay for angiogenesis factors: Reactions induced by carrier materials. Exp Pathol (Jena) 15:241–249.

Jimi S, Kohno K, Ono M, Kuwano M, Itagaki Y, and Ishikawa K (1995). Modulation by bovine angiogenin of tubular morphogenesis and expression of plasminogen activator in bovine endothelial cells. Biochem Biophys Res Commun 211: 476–483.

Kenyon BM, Browne F, and D'Amato RJ (1997). Effects of thalidomide and related metabolites in a mouse corneal model of neovascularization. Exp Eye Res 64:971–978.

Kenyon BM, Voest EE, Chen CC, Flynn E, Folkman J, and D'Amato RJ (1996). A model of angiogenesis in the mouse cornea. Invest Ophthalmol Vis Sci 37:1625–1632.

Kerstens HM, Poddighe PJ, and Hanselaar AG (1995). A novel in situ hybridization signal amplification method based on the deposition of biotinylated tyramine. J Histochem Cytochem 43:347–352.

Koolwijk P, van Erck MG, de Vree WJ, Vermeer MA, Weich HA, Hanemaaijer R, and van Hinsbergh VW (1996). Cooperative effect of TNFalpha, bFGF, and VEGF on the formation of tubular structures of human microvascular endothelial cells in a fibrin matrix: Role of urokinase activity. J Cell Biol 132: 1177–1188.

Kroon ME, Koolwijk P, van Goor H, Weidle UH, Collen A, van der Pluijm G, and van Hinsbergh VW (1999). Role and localization of urokinase receptor in the formation of new microvascular structures in fibrin matrices. Am J Pathol 154:1731–1742.

Kruger EA, Duray PH, Tsokos MG, Venzon DJ, Libutti SK, Dixon SC, Rudek MA, Pluda J, Allegra C, and Figg WD (2000). Endostatin inhibits microvessel formation in the ex vivo rat aortic ring angiogenesis assay. Biochem Biophys Res Commun 268:183–191.

Millauer B, Shawver LK, Plate KH, Risau W, and Ullrich A (1994). Glioblastoma growth inhibited in vivo by a dominant-negative Flk-1 mutant. Nature 367:576–579.

Montesano R, Mouron P, and Orci L (1985). Vascular outgrowth from tissue explants embedded in fibrin or collagen gels: A simple in vitro model of angiogenesis. Cell Biol Int Rep 9:869–875.

Moore BB, Keane MP, Addison CL, Arenberg DA, and Strieter RM (1998). CXC chemokine modulation of angiogenesis: The importance of balance between angiogenic and angiostatic members of the family. J Investig Med 46:113–120.

Neville LF, Mathiak G, and Bagasra O (1997). The immunobiology of interferon-gamma inducible protein 10 kD (IP-10): A novel, pleiotropic member of the C-X-C chemokine superfamily. Cytokine Growth Factor Rev 8:207–219.

Nicosia RF and Ottinetti A (1990). Growth of microvessels in serum-free matrix culture of rat aorta. A quantitative assay of angiogenesis in vitro. Lab Invest 63:115–122.

Nissanov J, Tuman RW, Gruver LM, and Fortunato JM (1995). Automatic vessel segmentation and quantification of the aortic ring assay of angiogenesis. Lab Invest 73:734–739.

Nissen NN, Polverini PJ, Koch AE, Volin MV, Gamelli RL, and DiPietro LA (1998). Vascular endothelial growth factor mediates angiogenic activity during the proliferative phase of wound healing. Am J Pathol 152:1445–1452.

O'Reilly MS, Boehm T, Shing Y, Fukai N, Vasios G, Lane WS, Flynn E, Birkhead JR, Olsen BR, and Folkman J (1997). Endostatin: An endogenous inhibitor of angiogenesis and tumor growth. Cell 88:277–285.

Pepper MS (1997). Manipulating angiogenesis. Arterioscler Thromb Vasc Biol 17:605–619.

Pepper MS and Montesano R (1990). Proteolytic balance and capillary morphogenesis. Cell Differ Dev 32:319–327.

Roeckl W, Hecht D, Sztajer H, Waltenberger J, Yayon A, and Weich HA (1998). Differential binding characteristics and cellular inhibition by soluble VEGF receptors 1 and 2. Exp Cell Res 241:161–170.

Rosengart TK, Lee LY, PAtel SR, Sanborn TA, Parikh M, Bergman GM, Hachamovich R, Szulc M, Kligfield PD, Okin PM, Hahn RT, Devereux RM, Post MR, Hackett NR, Foster T, Grasso TM, Lesser ML, Isom OW, and Crystal RG (1999). Angiogenesis gene therapy: Phase I assessment of direct intramyocardial administration of an adenovirus vector expressing VEGF121 cDNA to individuals with clinically significant severe coronary artery disease. Circulation 100:468–474.

Salvesen HB and Akslen LA (1999). Significance of tumour-associated macrophages, vascular endothelial growth factor and thrombospondin-1 expression for tumour angiogenesis and prognosis in endometrial carcinomas. Int J Cancer 84:538–543.

Sten-Linder M, Linder C, Strander H, Munck-Wikland E, Wersall P, Linder S, and Wiman B (1999). Angiostatin fragments in urine from patients with malignant disease. Anticancer Res 19:3409–3414.

Strieter RM, Kunkel SL, Arenberg DA, Burdick MD, and Polverini PJ (1995). Interferon gamma-inducible protein 10 (IP-10), a member of the C-X-C chemokine family, is an inhibitor of angiogenesis. Biochem Biophys Res Commun 210:51–57.

Strom SC and Michalopoulos G (1982). Collagen as a substrate for cell growth and differentiation. Methods Enzymol 82 Pt A:544–555.

Szabo S and Sandor Z (1998). The diagnostic and prognostic value of tumor angiogenesis. Eur J Surg Suppl 582:99–103.

Taddei L, Chiarugi P, Brogelli L, Cirri P, Magnelli L, Raugei G, Ziche M, Granger HJ, Chiarugi V, and Ramponi G (1999). Inhibitory effect of full-length human endostatin on in vitro angiogenesis. Biochem Biophys Res Commun 263:340–345.

Tamura H and Greenwald GS (1987). Angiogenesis and its hormonal control in the corpeus luteum of the pregnant rat. Biol Reprod 36:1149–1154.

Van Beek E, Van der Wee-Pals L, van de Ruit M, Nijweide P, and Lowik CWGM (1993). Leukemia inhibitory factor inhibits osteoclastic resorption, growth, mineralization, and alkaline phosphatase activity in fetal mouse metacarpal bones in culture. J Bone Miner Res 8:191–198.

van der Pluijm G, Lowik CWGM, de Groot H, Alblas MJ, van der Wee-Pals LJ, Bijvoet OL, and Papapoulos SE (1991). Modulation of PTH-stimulated osteoclastic resorption by bisphosphonates in fetal mouse bone explants. J Bone Miner Res 6:1203–1210.

Werb Z, Vu TH, Rinkenberger JL, and Coussens LM (1999). Matrix-degrading proteases and angiogenesis during development and tumor formation. APMIS 107:11–18.

Wojtowicz-Praga SM, Dickson RB, and Hawkins MJ (1997). Matrix metalloproteinase inhibitors. Invest New Drugs 15:61–75.

Yamaguchi N, Anand-Apte B, Lee M, Sasaki T, Fukai N, Shapiro R, Que I, Lowik C, Timpl R, and Olsen BR (1999). Endostatin inhibits VEGF-induced endothelial cell migration and tumor growth independently of zinc binding. EMBO J 18:4414–4423.

Zetter BR (1980). Migration of endothelial cells is stimulated by tumour-derived factors. Nature 5759:41–43.